This is a repository copy of *Free electron degeneracy effects on collisional excitation, ionization, de-excitation and three-body recombination*.

White Rose Research Online URL for this paper:
https://eprints.whiterose.ac.uk/102543/

Version: Accepted Version

Article:

Free electron degeneracy effects on collisional excitation, ionization, de-excitation and three-body recombination

G J Tallents

York Plasma Institute, Department of Physics, University of York, York YO10 5DD, U.K.

Abstract

Collisional-radiative models enable average ionization and ionization populations, plus the rates of absorption and emission of radiation to be calculated for plasmas not in thermal equilbrium. At high densities and low temperatures, electrons may have a high occupancy of the free electron quantum states and evaluations of rate coefficients need to take into account the free electron degeneracy. We demonstrate that electron degeneracy can reduce collisional rate coefficients by orders-of-magnitude from values calculated neglecting degeneracy. We show that assumptions regarding the collisional differential cross-section can alter collisional ionization and recombination rate coefficients by a further factor two under conditions relevant to inertial fusion.

Keywords: collisional radiative; NLTE; electron degeneracy; dense plasmas.

1. Introduction

The modeling of plasma ionization and radiative emission and absorption at high density is central to several aspects of inertial controlled fusion (ICF), short wavelenth free electron laser interactions with solids and in the modeling of stellar ionization. In ICF, hohlraum emission and the absorption of radiation in the fuel capsule walls [1], plus the diagnosis of mix of shell wall and fuel [2] depend on accurate calculations of plasma ionization and the plasma radiative properties. Flexible codes are used to post-process output from radiation-hydrodynamic and particle-in-cell codes to generate spectra and images for comparison to

experimental measurements [3], [4]. A double peak in the pressure profile of carbon shell material in the National Ignition Facility (NIF) point design due to carbon Li-like ions may have caused reduced neutron production [5]. ICF seeks to compress material at low temperatures (with pressures below 1.7 times Fermi degenerate [6]]) with high incident radiation flux (e.g. the spectrally integrated radiation flux in a NIF holhruam of temperature 300 eV approaches 10^{15}Wcm^{-2}). Under these conditions, we show that free electron degeneracy can have a significant effect on plasma ionization, emission and absorption.

Degeneracy effects are important in extreme ultraviolet (EUV) free electron laser interactions with solids where warm (< 10 eV) solid density plasma in the presence of strong photo-ionizing radiation is created [7], [8],[9]. For example, Aslanyan and Tallents [7] showed that for EUV irradiances of 10^{14} Wcm^{-2} and greater, plasma ionization is significantly affected by free electron degeneracy. Degeneracy reductions of three-body recombination rates may also be significant in hard x-ray free electron laser measurements of ionization rates [10]. Free electron degeneracy should affect the evaluation of the ionization of metal rich white dwarf stars [11]. A high radiation flux causes photo-ionization with three-body recombination acting as the dominant recombination process. We show here that three-body recombination is reduced by orders-of-magnitude due to free electron degeneracy.

Degeneracy effects are included in some collisional-radiative models [[4], [12], [13], [14],[15]]. However, the methods and rationale for treatment of degeneracy in collsional-radiative codes have not been explained in the literature and the accuracy and sensitivity of many of the modeling approximations have not been investigated . The role of free electron degeneracy in suppressing bremsstrahlung in inertial fusion has been discussed [16], [17]. Recently Scott [[18]] described approximate methods to evaluate the modification of rate coefficients by degeneracy effects. In this paper, we explain the methods and rationale for treatment of degeneracy in collisional-radiative codes in some detail and deduce the appropriate detailed balance relationships in degenerate plasmas. We extend the treatment by Scott to consider differential cross-sections for collisional ionization
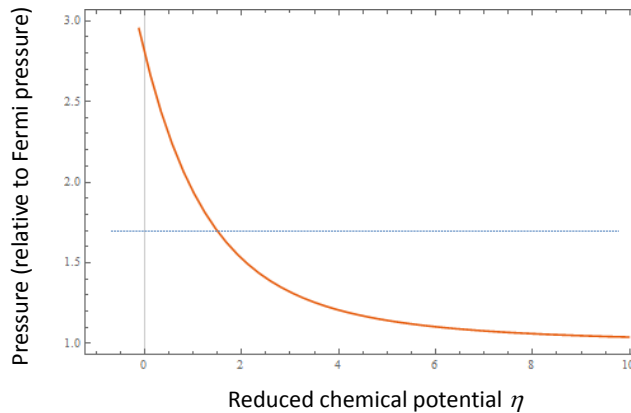
Figure 1: The total pressure of an electron gas including the degeneracy pressure as a function of reduced chemical potential. The horizontal line shows the maximum pressure for compression in inertial fusion design studies [[6]] .

and three-body recombination which are not constant with differing energies of the two free electrons. Our work shows the significant effect on collisional ionization and recombination rate coefficients of degeneracy effects associated with the distribution of the energies of the two free electrons.

2. Electron degeneracy

2.1. Background physics of electron degeneracy

The Pauli excluson principle requires that only one electron can occupy a quantum state. The principle applies to free electrons and bound electrons in a plasma so that the occupation of all quantum states is governed by Fermi-Dirac statistics, though at low densities average occupancy per quantum state is low for excited bound and free states so that simpler Boltzmann populations are accurately employed. In equilibirum at temperature T, the number N of electrons occupying an energy state E given by the Fermi-Dirac distribution is such that

3

$$N = \frac{g}{\exp\left(-\frac{\mu - E}{kT}\right) + 1} \tag{1}$$

where μ is the chemical potential, g is the degeneracy of quantum states at the energy E and k is Boltzmann's constant. By considering the density of free electron wave functions, it is possible to evaluate the number of free electron quantum states per unit volume. The number $g(E)dE$ of free electron quantum states with kinetic energy in the range E to $E+dE$ per unit volume is given by

$$g(E)dE = \frac{4}{\sqrt{\pi}}\left(\frac{2\pi m}{h^2}\right)^{3/2} E^{1/2}dE \tag{2}$$

where m is the electron mass and h is Planck's constant. Consequently, the free electron distribution function is given by

$$f(E) = g(E)N = \frac{4}{\sqrt{\pi}}\left(\frac{2\pi m}{h^2}\right)^{3/2} E^{1/2} \frac{1}{\exp\left(-\frac{\mu - E}{kT}\right) + 1}. \tag{3}$$

The chemical potential μ is the energy needed to add one more electron to the free electron population at constant entropy and volume. It is related to the electron density by the requirement that an integration of the electron distribution function over all energies gives the total free electron density N_e. We can write

$$N_e = \int_0^\infty f(E)dE = \frac{4}{\sqrt{\pi}}\left(\frac{2\pi mkT}{h^2}\right)^{3/2} I_{1/2}(\mu/kT) \tag{4}$$

where $I_m(\eta)$ is the Fermi-Dirac integral of order m. We introduce a reduced chemical potential $\eta = \mu/kT$ and write for the Fermi-Dirac integrals

$$I_m(\eta) = \int_0^\infty \frac{x^m dx}{\exp(x - \eta) + 1}. \tag{5}$$

In the low density limit where $\eta = \mu/kT << -1$, the Fermi-Dirac integral has an analytic solution with

$$I_{1/2}(\mu/kT) \approx \frac{\sqrt{\pi}}{2} \exp(\mu/kT).$$

Consequently at large negative chemical potential degeneracy effects become negligible and the chemical potential and electron density are related through

$$\exp\left(\frac{\mu}{kT}\right) = \frac{N_e}{2}\left(\frac{h^2}{2\pi mkT}\right)^{3/2}. \tag{6}$$

At large positive values of the chemical potential, the chemical potential μ approaches the Fermi energy E_F and equation 4) involves a simple integral of form

$$I_{1/2}(\eta) = \int_0^{E_F/kT} x^{1/2}dx$$

so that we find

$$E_F = \left(\frac{3}{8\pi}\right)^{2/3}\frac{h^2}{2m}N_e^{2/3}. \tag{7}$$

We can evaluate the internal electron energy by an integral of form

$$U = \int_0^\infty Ef(E)dE = \frac{4}{\sqrt{\pi}}\left(\frac{2\pi mkT}{h^2}\right)^{3/2} kT \ I_{3/2}(\mu/kT). \tag{8}$$

At high positive chemical potential, the Fermi internal energy $U_F = (3/5)N_e E_F$. The ratio of the internal energy U to the Fermi internal energy U_F gives the ratio of the pressure to the Fermi pressure (see figure (1).

2.2. Deriving the Saha equation

In the ionization process of converting a Z charged ion to a $Z+1$ charged ion, a free electron with energy (say E) is created and a $Z+1$ ion quantum state is populated. We assume that a particular $Z+1$ charge quantum state has a probability P of existing. In a low density plasma with low occupancy of quantum states by the electrons, P approaches unity, but we shall see later that in a degenerate plasma, the probability that the state can exist is less than unity. For example, in the limit of T approaching zero and the number of bound states after allowing for the effect of continuum lowering being sufficiently large, all electrons simply fill up the bound quantum states of the lowest charged state and $P = 0$. This lack of ionization of a fully degenerate plasma was first noted by

5

Chandrasekhar [19]. In practise, ionization at high electron degeneracy becomes dependent on ionization depression (continuum lowering) due to the perturbing effects of nearby ions and the electron gas (see e.g. [20]) which reduces the number of available bound quantum states.

The population ratio of the free electron number density $f(E)dE$ and the population N_Z of bound electrons of charge Z per unit volume can be found using equation (1) after allowing for the degeneracy of the free electrons (given by equation (2)) and the degeneracy g_Z of the bound quantum state. For each $Z + 1$ ion, there are $g(E)dE/N_{Z+1}$ free electron states, where N_{Z+1} is the number density of $Z + 1$ ionization states. The bound state of the $Z + 1$ ion may also be degenerate with degeneracy g_{Z+1}, so that the total degeneracy of the 'upper state' created by ionization is $g_{Z+1}g(E)dE/N_{Z+1}$. The ratio of the Fermi-Dirac populations for the free electrons $f(E)dE$ and bound electrons N_Z can be written as a ratio of the 'upper' and 'lower' state populations using equation (1). We have

$$\frac{f(E)dE}{N_Z} = \frac{g_{Z+1}g(E)dE/N_{Z+1}}{g_Z} \frac{\exp[-(\mu + E_{ion})/kT] + 1}{\exp[-(\mu - E))/kT] + 1} P. \tag{9}$$

Here E_{ion} is the ionization energy of the Z charged ion quantum state being considered. ionization energy is negative on our free electron energy scale, hence our assumed positive E_{ion} has the opposite sign to the free electron kinetic energy E in equation (9). The value of E_{ion} should include a calculation of the continuum lowering effect [20].

If we integrate both sides of equation (9), we obtain

$$N_e = \frac{N_Z}{N_{Z+1}} \frac{g_{Z+1}}{g_Z} \frac{4}{\sqrt{\pi}} \left(\frac{2\pi mkT}{h^2}\right)^{3/2} \left[\exp\left(-\frac{\mu + E_{ion}}{kT}\right) + 1\right] I_{1/2}(\mu/kT)P \tag{10}$$

if P is independent of energy E. Using the definition of the chemical potential (equation (4)), equation (10) reduces to

$$\frac{N_{Z+1}}{N_Z} = \frac{g_{Z+1}}{g_Z} \left[\exp\left(-\frac{\mu + E_{ion}}{kT}\right) + 1\right] P. \tag{11}$$

2.3. The Saha equation

The existence of a $Z + 1$ charged quantum state depends on the number of 'holes' in the Z charged ion i.e. the number of states not fully occupied. For example, if all the quantum states of the Z charged ion are occupied, no electrons have been removed to create the $Z + 1$ charge ion, so the probability P that the $Z + 1$ state exists is zero. More generally, considering ionization from a quantum state with ionization potential E_{ion} we can write

$$P = 1 - \frac{1}{\exp\left(-\frac{\mu + E_{ion}}{kT}\right) + 1}. \tag{12}$$

P has the form of a 'blocking factor' representing the probability that the bound state of ionization energy E_{ion} has a 'hole' or quantum state which is unfilled. The number of holes determines the probability that an electron has been removed to produce a $Z + 1$ quantum state. Substituting this expression for P into equation (11) gives

$$\frac{N_{Z+1}}{N_Z} = \frac{g_{Z+1}}{g_Z} \exp\left(-\frac{E_{ion}}{kT}\right) \exp\left(-\frac{\mu}{kT}\right). \tag{13}$$

This expression for the Saha ionization balance is consistent with a thermodynamic understanding of ionization where the energy of the free electrons changes by the ionization energy plus the chemical potential $(E_{ion} + \mu)$ upon ionization. The chemical potential is defined as the energy required to add one more electron to the free electron population. If we substitute the low density limit (equation 6) for the chemical potential, we obtain an expression often cited for the Saha equation. We get

$$\frac{N_e N_{Z+1}}{N_Z} = \frac{g_{Z+1}}{g_Z} 2 \left(\frac{2\pi mkT}{h^2}\right)^{3/2} \exp\left(-\frac{E_{ion}}{kT}\right). \tag{14}$$

If we assume that the probability P for the existence of the $Z + 1$ quantum state is as given by equation(12), then the ratio of the populations N_2 and N_1 of two bound states with ionization energies E_2 and E_1 and degeneracies g_2 and g_1 from equation (13) is given by

$$\frac{N_2}{N_1} = \frac{g_2}{g_1} \exp\left(-\frac{E_2 - E_1}{kT}\right) \tag{15}$$

as the term involving the chemical potential cancels. This Boltzmann ratio (equation (15)) is the same as found at low densities where free electron degeneracy is not important.

3. Expressions for rate coefficients with degeneracy

To evaluate rate coefficients for collisional processes, we need to integrate the cross-section for the appropriate process over the range of free-electron energies taking account of blocking factors to allow for electron degeneracy. Cross-sections $\sigma(E)$ are often tabulated in the form of a collision strength $\Omega(E)$ [[21]] such that

$$\sigma(E) = \frac{\Omega(E) \ \pi a_0^2}{g \ E} \tag{16}$$

where πa_0^2 is a cross-section for the ground state of the hydrogen atom (taken as the area associated with the Bohr radius a_0) and g is the degeneracy of the initial state. The collision strength has been shown in many studies to vary slowly with the electron energy E and consequently is tabulated in databases rather than absolute cross-sections (see. e.g. [22],[23]). The 'effective collision strength' $\Omega(E)$ averaged over a Maxwellian distribution of electron energies is found to vary even more slowly with electron temperature. We are interested in gauging the effect of degeneracy, so we assume in this section that the cross-sections vary as $1/E$. Following equation (16), we write cross-sections as

$$\sigma(E) = \Phi \frac{\sigma(E_{th}) E_{th}}{E} \tag{17}$$

where E_{th} is the threshold or minimum electron energy needed to cause the collisional transition and $\Phi = 1$. The collision strength concept was introduced for collisional excitation, but is applicable for collisional ionization. For section 4, Φ can take any value, so the analysis is independent of the form of the cross-section, while in section 5, we introduce a differential cross-section for collisional ionization which varies with the ejected electron energy.

8

3.1. Collisional excitation

Including the effects of degeneracy, the transition rate per ion for collisional excitation from ionization energy E_1 to E_2 is given by

$$K_{12}N_e = \int_{\Delta E}^{\infty} (2E/m)^{1/2}\sigma_{12}(E)f(E)\ P(E-\Delta E)\ dE \tag{18}$$

where the blocking factor P is calculated for the final free electron energy $E - \Delta E$, where E is the initial electron energy and $\Delta E = E_2 - E_1$. We have

$$P(\epsilon) = 1 - \frac{1}{\exp\left(-\frac{\mu-\epsilon}{kT}\right)+1} \tag{19}$$

and the free electron distribution $f(E)$ is given by equation (3). In equation (18), $\sigma_{12}(E)$ is the cross-section for the collsional transition between bound states.

Following equation (17), equation (18 can be written as

$$K_{12}N_e \approx \frac{4}{\sqrt{\pi}}\left(\frac{2\pi m}{h^2}\right)^{3/2}\left(\frac{2}{m}\right)^{1/2}\Delta E\ \sigma_{12}(\Delta E)\ J_{12}(\Delta E)\ kT \tag{20}$$

where

$$J_{12}(\Delta E) = \int_{\Delta E/kT}^{\infty} \frac{1}{\exp\left(-\frac{\mu-E}{kT}\right)+1}\left(1 - \frac{1}{\exp\left(-\frac{\mu-E+\Delta E}{kT}\right)+1}\right) dE/kT$$
$$= \frac{\exp(-\Delta E/kT)}{1 - \exp(-\Delta E/kT)}\ln\left[\frac{1+\exp(\mu/kT)}{1+\exp((\mu-\Delta E)/kT)}\right]. \tag{21}$$

In the absence of degeneracy, the integral $J_{12}(\Delta E)$ simplifies to

$$J_{12}(\Delta E) = \int_{\Delta E/kT}^{\infty} \exp((\mu-E)/kT)dE/kT = \exp((\mu-\Delta E)/kT) \tag{22}$$

which means that the ratio R_{12} of the collisional excitation rate coefficient with degeneracy to the rate coefficient without degeneracy is given by

$$R_{12} = \frac{\exp(-\mu/kT)}{1 - \exp(-\Delta E/kT)}\ln\left[\frac{1+\exp(\mu/kT)}{1+\exp((\mu-\Delta E)/kT)}\right]. \tag{23}$$

9

For a degenerate plasma, it is worth examining the relationship between excitation and de-exciation explicitly. The microreversibility condition for collisional excitation and de-excitation relates the cross-sections by the Klein-Rosseland relation [24], so that

$$\sigma_{21}(E) = \frac{g_1}{g_2} \frac{E + \Delta E}{E} \sigma_{12}(E + \Delta E) \tag{24}$$

where $\sigma_{21}(E)$ is the cross-section for collisional de-excitation. We can write out the expression for the collisional de-excitation rate coefficient K_{21} in a similar way to the construction of equation (18). We have

$$K_{21} N_e = \int_0^\infty (2E/m)^{1/2} \sigma_{21}(E) f(E) \, P(E + \Delta E) \, dE \tag{25}$$

where $P(E + \Delta E)$ is a blocking factor for the final energy of the colliding electron. Substituting equation (24), we have

$$K_{21} N_e = \int_0^\infty (2E/m)^{1/2} \frac{g_1}{g_2} \frac{E + \Delta E}{E} \sigma_{12}(E) f(E) \, P(E + \Delta E) \, dE.$$

Assuming as before for collisional excitation that the cross-section for collisional excitation varies approximately linearly with the inverse of energy (i.e. $\sigma_{12}(E + \Delta E) \propto \sigma_{12}(\Delta E)/(E + \Delta E)$), we can write that

$$K_{21} N_e \approx \frac{4}{\sqrt{\pi}} \left(\frac{2\pi m}{h^2} \right)^{3/2} \left(\frac{2}{m} \right)^{1/2} \frac{g_1}{g_2} \Delta E \; \sigma_{12}(\Delta E) \; J_{21}(\Delta E) \; kT \tag{26}$$

where

$$J_{21}(\Delta E) = \int_0^\infty \frac{1}{\exp\left(-\frac{\mu - E}{kT}\right) + 1} \left(1 - \frac{1}{\exp\left(-\frac{\mu - E + \Delta E}{kT}\right) + 1} \right) dE/kT \tag{27}$$

$$= \frac{1}{1 - \exp(-\Delta E/kT)} \ln \left[\frac{1 + \exp(\mu/kT)}{1 + \exp((\mu - \Delta E)/kT)} \right].$$

In the absence of degeneracy, we have that

$$J_{21}(\Delta E) = \int_0^\infty \exp((\mu - E)/kT) dE/kT = \exp(\mu/kT) \tag{28}$$

10

The ratio R_{21} of the collisional de-excitation rate coefficient with degeneracy to the coefficient without degeneracy is consequently identical to the ratio R_{12} for collisional excitation (see equation (23)). Finding these ratios to be equal shows the detailed balance relationship between K_{21} and K_{12} is independent of the chemical potential (and hence degree of degeneracy).

In order to illustrate further that collisional excitation and de-exciation are independent of the chemical potential, we can briefly consider when collisional excitation is balanced by collisional de-excitation. We can undertake this balance for a plasma with populations affected by degeneracy by invoking the concept of a blocking factor P, which is the probability of finding a 'hole' in the destination quantum population. The blocking factor takes an identical form to equation (12).

Consider collisional excitation from a lower level of population N_1 with ionisation energy E_1 to an upper excited level of population N_2 with ionisation E_2 with collisional excitation rate coefficient K_{12} and de-excitation rate coefficient K_{21}. We write

$$N_e K_{12} N_1 P(E_1) = N_e K_{21} N_2 P(E_2) \tag{29}$$

where $P(E_{ion})$ is the blocking factor for the state of ionisation energy E_{ion}. Using the Fermi-Dirac population ratio for N_1/N_2 (equation (1)) and the blocking factor expressions (equation (12)), we find that the collisional de-excitation rate coefficient is related to the collisional excitation rate coefficient for a degnerate plasma by

$$K_{21} = \frac{g_1}{g_2} \exp\left(\frac{E_2 - E_1}{kT}\right) K_{12}. \tag{30}$$

where g_1 and g_2 are the degeneracies of the lower and upper bound quantum states respectively. This is exactly the detailed balance relationship found at low densities where degeneracy is not important.

3.3. Collisional ionization

The collisional ionization rate coefficient K_{ion} evaluation requires a knowledge of the differential cross-section $\sigma(E, E_1)$ where we assume, say, that the incident electron has an energy E and the ejected electrons have energy E_1 and $E_2 = E - E_1 - E_{ion}$. We can write that

$$K_{ion}N_e$$

$$= \int_{E_{ion}}^{\infty} \left(\frac{2E}{m}\right)^{1/2} f(E) \left[\frac{\int_0^{E-E_{ion}} \sigma(E, E_1) \, P(E_1) \, P(E - E_1 - E_{ion}) \, dE_1}{\int_0^{E-E_{ion}} dE_1}\right] dE$$

$$(31)$$

where the blocking factors $P(E_1)$ and $P(E - E_1 - E_{ion})$ are appropriate for the two ejected electrons. We assume that the initial bound state has an ionization energy of E_{ion}. The integrations in the square bracket average the differential cross-section and blocking factors over the range of ejected electron energies (from zero energy to the impinging electron energy minus the ionization energy). As the two electrons in collisional ionization are indistinguishable, the differential cross-section $\sigma(E, E_1)$ is symmetric around energy $(E - E_{ion})/2$, so for enhanced computational speed, it possible to evaluate the integrals over the reduced range 0 to $(E - E_{ion})/2$ (see e.g. [[25]]). However, initially in this section we assume that the differential cross-section does not vary at all with the ejected electron energy E_1 and for clarity we will write the integral over the full range throughout.

If we assume as a first treatment that the differential cross-section is constant with ejected electron energy E_1 and simply varies as $\sigma(E, E_1) = \sigma(E_{ion}, 0)E_{ion}/E$ (see equation 17), we can proceed with a a similar approximation as we made for collisional excitation. In section (5), we return to consider more realistic differential cross-sections where one electron typically has a much greater energy than the other. However, with the assumption that the differential cross-section is independent of the energy distribution between the two electrons, the rate coefficient can be written as

$$K_{ion} N_e \approx \frac{4}{\sqrt{\pi}} \left(\frac{2\pi m}{h^2} \right)^{3/2} \left(\frac{2}{m} \right)^{1/2} E_{ion} \ \sigma(E_{ion}, 0) \ J_{ion}(E_{ion}) \ (kT) \qquad (32)$$

with

$$J_{ion}(E_{ion}) = \int_{E_{ion}}^{\infty} \frac{1}{\exp\left(-\frac{\mu - E}{kT} \right) + 1} \ \frac{1}{E - E_{ion}}$$

$$\left[\int_{0}^{\frac{E - E_{ion}}{kT}} \left(1 - \frac{1}{\exp\left(-\frac{\mu - E_1}{kT} \right) + 1} \right) \left(1 - \frac{1}{\exp\left(-\frac{\mu - E + E_1 + E_{ion}}{kT} \right) + 1} \right) d(\frac{E_1}{kT}) \right] dE.$$
$$(33)$$

The integral in the square brackets is over the blocking factors for the two electrons after the collision. Letting $y = (E - E_{ion})/kT$ and $\eta = \mu/kT$, the integral can be re-written and solved analytically, so that

$$J_{ion}^*(y) = \frac{1}{y} \int_0^y \left(1 - \frac{1}{\exp(-\eta + x) + 1} \right) \left(1 - \frac{1}{\exp(-\eta + y - x) + 1} \right) dx \quad (34)$$

$$= \frac{1}{1 - \exp(2\eta - y)} \left[1 + \frac{2}{y} \ln \left(\frac{e^{\eta - y} + 1}{e^{\eta} + 1} \right) \right].$$

The double integral is not analytically soluble. We can write for $J_{ion}(E_{ion})$ that

$$J_{ion}(E_{ion}) = \int_0^{\infty} J_{ion}^*(y) \frac{1}{e^{-\eta + y + \beta} + 1} dy \qquad (35)$$

where $\beta = E_{ion}/kT$.

For non-degenerate free electrons, the solution of equation (33) is

$$J_{ion}(E_{ion}) = \exp \left(\frac{\mu - E_{ion}}{kT} \right) \qquad (36)$$

For non-degenerate electrons, we define a ratio R_{ion} for the value of $J_{ion}(E_{ion})$ relative to the low degeneracy value. We have

$$R_{ion} = J_{ion}(E_{ion}) / \left[\exp \left(\frac{\mu - E_{ion}}{kT} \right) \right]. \qquad (37)$$

Substituting into equation (32) using the non-degenerate expression for $\exp(\mu/kT)$ (equation (6)) gives
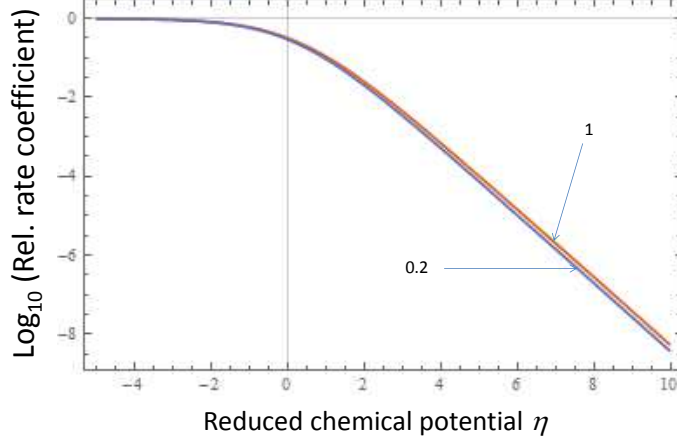
Figure 2: The ratio R_{ion} of the degenerate rate coefficient for ionization (assuming a constant differential cross-section) to the rate coefficient calculated assuming the electrons are non-degenerate. Curves for different ionization energy relative to the electron temperature (β) are labelled.

$$K_{ion} \approx \frac{2}{\sqrt{\pi}} \left(\frac{2}{m} \right)^{1/2} \frac{E_{ion}}{(kT)^{1/2}} \sigma(E_{ion}, 0) \exp\left(-\frac{E_{ion}}{kT} \right). \tag{38}$$

We plot the ratio R_{ion} of the degenerate rate coefficient to the rate coefficient calculated assuming the electrons are non-degenerate in figure (2). The ionization rate coefficient changes by several orders-of-magnitude at high positive chemical potential, but the change is almost independent of the electron temperature for a constant value of the reduced chemical potential.

3.4. Collisional recombination

The inverse process to collisional ionization is collisional recombination. Here, there are intitially two free electrons (we assume with energy E_1 and E_2) and a $Z+1$ charged ion. As three particles are involved, collisional recombination is often called three-body recombination. After the collisional process, there is one free electron (we assume with energy E) and a Z charged ion. The

differential cross-section $\sigma(E_1, E)$ for the collisional recombination of an electron is needed. The rate coefficient K_{rec} for collisional recombination including the effects of degeneracy can be written as

$$K_{rec}N_e = (2/m) \int_{E_{ion}}^{\infty} \left[\frac{\int_0^{E-E_{ion}} \sqrt{E_1}f(E_1)\sqrt{E_2}f(E_2)\sigma(E_1,E)dE_1}{\int_0^{E-E_{ion}} dE_1} \right] P(E)dE \tag{39}$$

where now $E_2 = E - E_1 - E_{ion}$. The integrations in the square bracket average the differential cross-section over the possible initial distributions of the free electrons. Only one blocking factor $P(E)$ is involved for the final free electron of energy E.

The microreversibility condition for collisional ionization and recombination is known as the Fowler relation [24] and is given by

$$\sigma(E_1, E) = \frac{g_Z}{g_{Z+1}} \sqrt{\frac{m}{2}} \left[\frac{4}{\sqrt{\pi}} \left(\frac{2\pi m}{h^2} \right)^{3/2} \right]^{-1} \frac{E}{E_1 E_2} \sigma(E, E_1). \tag{40}$$

The expression is complicated by the need to allow for a measure of the degeneracy for the free electron created by ionization (the quantity in the square bracket, see equation (2)). As we have done previously, we assume that the differential cross-section for collisional ionization is independent of the different electron energies E_1 and E_2 and varies as $\sigma(E, E_1) = \sigma(E_{ion}, 0)E_{ion}/E$. Using the microreversibility relationship between collisional ionization and recombination, we obtain that

$$K_{rec}N_e \approx \frac{4}{\sqrt{\pi}} \left(\frac{2\pi m}{h^2} \right)^{3/2} \left(\frac{2}{m} \right)^{1/2} \frac{g_Z}{g_{Z+1}} E_{ion} \, \sigma(E_{ion}, 0) \, J_{rec}(E_{ion}) \, (kT) \tag{41}$$

with

$$J_{rec}(E_{ion}) =$$

$$\int_{E_{ion}}^{\infty} \left[\int_0^{\frac{E-E_{ion}}{kT}} \left(\frac{1}{\exp\left(-\frac{\mu-E_1}{kT}\right)+1} \right) \left(\frac{1}{\exp\left(-\frac{\mu-E+E_1+E_{ion}}{kT}\right)+1} \right) d\left(\frac{E_1}{kT} \right) \right]$$

15

$$\frac{1}{E - E_{ion}} \left[1 - \frac{1}{\exp\left(-\frac{\mu - E}{kT}\right) + 1} \right] dE \tag{42}$$

The integral within the square bracket represents the averaging of the occupancy of the two electrons present before the collision. Letting $y = (E - E_{ion})/kT$ and $\eta = \mu/kT$, the integral can be re-written and solved analytically, so that

$$J^*_{rec}(y) = \frac{1}{y} \int_0^y \left(\frac{1}{\exp(-\eta + x) + 1} \right) \left(\frac{1}{\exp(-\eta + y - x) + 1} \right) dx \tag{43}$$

$$= \frac{1}{\exp(-2\eta + y) - 1} \left[1 + \frac{2}{y} \ln\left(\frac{e^{\eta - y} + 1}{e^{\eta} + 1} \right) \right].$$

We can write that

$$J_{rec}(E_{ion}) = \int_0^\infty J^*_{rec}(y) \left(1 - \frac{1}{e^{-\eta + y + \beta} + 1} \right) dy \tag{44}$$

where $\beta = E_{ion}/kT$.

In the limit of low degeneracy, equation (42) becomes equal to $\exp(2\eta) = \exp(2\mu/kT)$. The ratio R_{rec} of the collisional recombination rate including degeneracy to that without degeneracy can be written as

$$R_{rec} = \frac{J_{rec}(E_{ion})}{e^{2\eta}}.$$

Using the above equations (43, 44), it is straightforward to show that $R_{rec} = R_{ion}$, where R_{ion} is the ratio of the rate coefficient for collisional ionization with degeneracy to the rate coefficient without degeneracy (see equation (37)).

4. The detailed balance relationship for collisional ionization and recombination

Following equation (17), we can express quite generatlly the differential cross-section for collisional ionization as

$$\sigma(E, E_1) = \Phi \, \sigma_{tot}(E_{ion}) E_{ion}/E \tag{45}$$

16

where Φ represents the variation of the differential cross-section with different values of the energy E_1 of an electron ejected during collisional ionization. The cross-section $\sigma_{tot}(E_{ion})$ represents the threshold value of the cross-section where the incident electron has energy $E = E_{ion}$. Equation (45) is equivalent to the collision strength approach so that, in principle, Φ can vary with the incident electron energy E as well as the energy split between the two electrons produced in ionization (energies E_1 and E_2). The rate coefficient for collisional ionization is then given by equation (32) with

$$J_{ion} = \int_0^\infty \int_0^y \frac{\Phi}{y} \left(1 - \frac{1}{e^{-\eta+x}+1}\right) \left(1 - \frac{1}{e^{-\eta+y-x}+1}\right) \left(\frac{1}{e^{-\eta+y+\beta}+1}\right) dx\, dy \tag{46}$$

Similarly, the rate coefficient for collisional three-body recombination is given by equation (41) with

$$J_{rec} = \int_0^\infty \int_0^y \frac{\Phi}{y} \left(\frac{1}{e^{-\eta+x}+1}\right) \left(\frac{1}{e^{-\eta+y-x}+1}\right) \left(1 - \frac{1}{e^{-\eta+y+\beta}+1}\right) dx\, dy \tag{47}$$

It is relatively straightforward to show that $J_{ion} = e^{-\eta-\beta} J_{rec}$ for any variation of Φ. This means that we can write quite generally that

$$\frac{K_{ion}}{K_{rec}} = \frac{g_{Z+1}}{g_Z} \frac{J_{ion}}{J_{rec}} = \frac{g_{Z+1}}{g_Z} \exp\left(-\frac{\mu}{kT}\right) \exp\left(-\frac{E_{ion}}{kT}\right). \tag{48}$$

The right hand side of equation (48) is, of course, the Saha ratio of populations N_{Z+1}/N_Z (see equation 13).

5. Ionization rate coefficient calculation using the Mott differential cross section

So-far we have assumed that the differential cross-section in collisional ionization and three-body recombination is constant with different energy values of the two free electrons. Experimentally, it is found that the differential cross-section is greater where one electron has more energy. The Mott differential

17

cross-section has been found to be a good fit to many experimental measurements [26], [27]. The Mott differential cross section can be written as follows [28]

$$\sigma(E, E_1) = \frac{4\pi a_0^2 R_g^2}{E} \left[\frac{1}{(E_1 + E_{ion})^2} + \frac{1}{(E_1 - E)^2} - \frac{1}{(E_1 + E_{ion})(E_1 - E)} \right] \tag{49}$$

where a_0 is the Bohr radius, R_g is the Rydberg constant (13.6 eV) and E_1 and E_2 are the energies of the two free electrons created in collisional ionization. The energy E represents the energy of the incident electron creating the ionization and, as before, E_{ion} is the ionization energy. Following equation (31) we can write for the value of the collisional ionization rate coefficient that

$$K_{ion} N_e \approx \frac{4}{\sqrt{\pi}} \left(\frac{2\pi m}{h^2} \right)^{3/2} \left(\frac{2}{m} \right)^{1/2} 4\pi a_0^2 R_d^2 \, L_{ion}(E_{ion}) \frac{1}{kT} \tag{50}$$

with

$$L_{ion}(E_{ion}) = \int_{E_{ion}}^{\infty} \frac{1}{\exp\left(-\frac{\mu - E}{kT}\right) + 1} \frac{1}{E - E_{ion}}$$

$$\int_0^{\frac{E - E_{ion}}{kT}} \left[\frac{1}{(E_1 + E_{ion})^2} + \frac{1}{(E_1 - E)^2} - \frac{1}{(E_1 + E_{ion})(E_1 - E)} \right] \tag{51}$$

$$\left(1 - \frac{1}{\exp\left(-\frac{\mu - E_1}{kT}\right) + 1} \right) \left(1 - \frac{1}{\exp\left(-\frac{\mu - E + E_1 + E_{ion}}{kT}\right) + 1} \right) d(\frac{E_1}{kT}) dE.$$

We can write out the integrals in terms of reduced parameters: ionization energy $\beta = E_{ion}/kT$, chemical potential $\eta = \mu/kT$, the ejected electron energy $x = E_1/kT$ and a measure of the incident electron energy $y = (E - E_{ion})/kT$. We have

$$L_{ion}(E_{ion}) = \int_0^{\infty} L_{ion}^*(y) \frac{1}{e^{-\eta + y + \beta} + 1} dy \tag{52}$$

with

$$L_{ion}^*(y) = \frac{1}{y} \int_0^y \left[\frac{1}{(x + \beta)^2} + \frac{1}{(x - y - \beta)^2} - \frac{1}{(x + \beta)(x - y - \beta)} \right]$$

$$\left(1 - \frac{1}{\exp(-\eta + x) + 1} \right) \left(1 - \frac{1}{\exp(-\eta + y - x) + 1} \right) dx. \tag{53}$$

18

In the absence of degeneracy when $\eta << -1$, equation (53) can be solved analytically so that

$$L_{ion}^* = \frac{2}{\beta(\beta + 1)} + \frac{2}{(2\beta + y)y} \ln(1 + y/\beta) \qquad (54)$$

The effect of utilising the Mott differential cross section to evaluate the colli-
340   sional ionization rate coefficient is illustrated in figure (3). The relative rate
coefficient calculated using the Mott differential cross-section is plotted relative
to the rate coefficient assuming a differential cross-section which is constant for
different values of the free electron energies E_1 and E_2. We have evaluated
$L_{ion}(E_{ion})$ (equation (52) divided by the same integral if degeneracy affects are
345   unimportant ($\eta << -1$, using equation (54) and then divided by the same ratio
R_{ion} given by equation(37). We see that at the reduced chemical potentials rel-
evant to ICF ($\eta > 1.5$, see figure (1)), the ionization rate coefficients are reduced
by at least a factor of two. Using detailed balance, a similar reduction occurs
in the rate of three-body recombination.

350   **6. Conclusion**

We have shown that the free electron degeneracy of high density, low temper-
ature plasmas can reduce collisional rate coefficients by orders-of-magnitude. We
have further shown that realistic Mott differential cross-sections further reduce
collisional ionization and three-body recombination rate coefficients when com-
355   pared to rate coefficients calculated assuming differential cross-sections which
are constant with the energies of the two free electrons involved in collisional
ionization and three-body recombination. These reductions in rate coefficients
become important in plasmas where excitation and ionization processes are not
in balance: for example, in inertial fusion, extreme ultra-violet and X-ray free
360   electron laser (FEL) interactions and in white dwarf stars. Here, radiative exci-
tation and ionization can be in balance with collisional de-excitation and three-
body recombination.The collisional de-excitation and three-body recombination
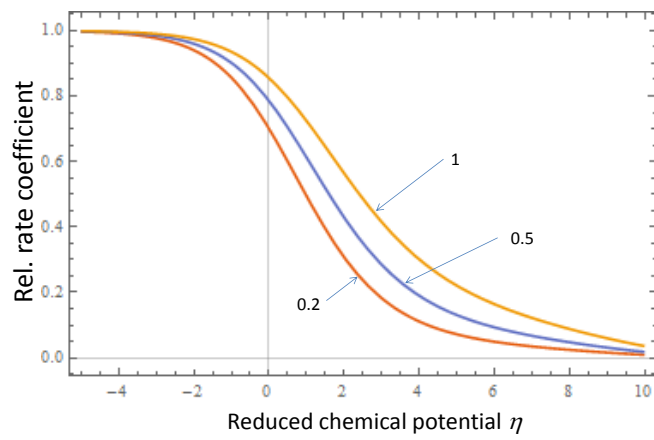effects are more affected by the electron degeneracy than photo-excitation and

19

Figure 3: The ratio of the ionization rate assuming a non-uniform differential cross-section as determined by Mott and a uniform differential cross-section for collisional ionization as a function of chemical potential. The ionization energy relative to the electron temperature (β) is labelled on the figure.

-ionization. When degeneracy effects are important, the ionization rate of the plasmas will be significantly enhanced (for example, as seen in XFEL interaction work[10]).

We have determined methods to calculate inverse rate coefficients and shown how the collisional excitation/de-excitation and ionization/recombination rate coefficients are universally related by the Saha equation when written in terms of the free-electron chemical potential. There are many uncertainties in collisional-radiative modeling of dense plasmas related particularly to the correct evaluation of all bound-bound processes (involving detailed calculation of ionic structure) and the evaluation of accurate cross-sections for collisional and radiative processes. We have shown that free-electron degeneracy effects may have a major effect on the correct evaluation of ionization in dense plasmas, yet relatively straightforward corrections to rate coefficients can be made.

Acknowledgements

References

[1] O. A. Hurricane et al, Fuel gain exceeding unity in an inertially confined fusion implosion, Nature 506 (2014) 438–438.

[2] S. P. Regan et al, Hot-spot mix in ignition-scale inertial confinement fusion targets, Phys. Rev. Lett. 111 (2013) 045001.

[3] J. J. MacFarlane, I. E. Golvkin, P. Want, P. R. Woodruff and N. A.Pereyra, SPECT3D a multi-dimensional collisional-radiative code for generating

₃₉₀ diagnostic signatures based on hydrodynamics and PIC simulation output, High Energy Density Physics 3 (2007) 181– 190.

[4] H. A. Scott and S. B. Hansen, Advances in NLTE modeling for integrated simulations, High Energy Density Physics 6 (2010) 39–47.

[5] Y. T. Dittrich et al, Design of a high-foot high adiobat ICF capsule for the national ignition facility, Phys. Rev. Lett. 112 (2014) 055002.

[6] S. W. Haan et al, Point design targets, specifications, and requirements for the 2010 ignition campaign on the national ignition facility, Phys. Plasmas 18 (2011) 051001.

[7] V. Aslanyan, G. Tallents, Ionization rate coefficients in warm dense plasmas, Phys. Rev. E 91 (6) (2015) 063106. `doi:10.1103/PhysRevE.91. 063106.`

[8] B. Deschaud, O. Peyrusse and F . B. Rosmej, Generalized atomic processes for interaction of intense femtosecond xuv- and x-ray radiation with solids, EPL 108 (2014) 53001. `doi:10.1209/0295-5075/108/53001.`

[9] B. Deschaud, O. Peyrusse and F . B. Rosmej, Atomic kinetics for isochoric heating of solid aluminum under short intense xuv free electron laser irradiation, High Energy Density Physics 15 (2015) 22–29. `doi: 10.1016/j.hedp.2015.03.007.`

[10] S. M. Vinko et al, Investigation of femtosecond collisional ionization rates in a solid-density aluminium plasma, Nature Comm. 6 (2015) 6397. `doi: 10.1038/ncomms7397.`

[11] T. Lanz and I. Hubeny, Non-LTE line-blanketed model atmospheres of hot stars .2. hot, metal-rich white-dwarfs, Astrophys. J 439 (1995) 905–916. `doi:10.1038/ncomms7397.`

[12] H. K. Chung, W. L. Morgan and R. W. Lee, FLYCHK: an extension to the K-shell spectroscopy kinetics model FLY, J. Quant. Spect. Rad. Trans. 81 (2003) 107–115.

[13] S. J. Rose, Degeneracy effects on photoionization in the solar interior, J. Phys. B. 26 (1993) L29–34.

[14] V. G. Molinari, D. Mostacci, F. Rocchi and M. Sumini, Quantum degeneracy corrections to plasma line emission and to Saha equation, Phys. Lett. A 316 (2003) 247–251.

[15] V. Aslanyan A. G. Aslanyan and G. J. Tallents, Efficient caclulation of degenerate atomic rates by numerical quadrature on GPUs submitted for publication, Computer Physics Commun.

[16] P. T. Leon, S. Eliezer and J. A. Martinez-Val, Advances in NLTE modeling for integrated simulations, Phys. Lett. A 343 (2005) 181–189.

[17] Y. D. Jung, Influence of the electron-exchange and quantum shielding on the bremsstrahlung spectrum in degenerate quantum plasmas, Physics Plasmas 20 (2013) 103302.

[18] H. A. Scott, Modern methods in collisional-radiative modeling of plasmas, Springer Verlag Series on Atomic, Optical and Plasma Physics, Berlin, pp 81-104, 2016.

[19] S. Chandrasekhar, The ionization formula and the new statistics, Phil. Mag. 9 (1930) 292.

[20] S. M. Vinko, O. Ciricosta and J. S. Wark, Density functional theory calculations of continuum lowering in strongly coupled plasmas, Nature Comm. 5 (2014) 3533. `doi:10.1038/ncomms4533`.

[21] D. Salzmann, Atomic physics in hot plasmas, (Oxford Univ. Press: Oxford) (1998) 102.

[22] H. L. Zhang, D. H. Sampson and A K Mohanty, Fully relativistic and quasirelativistic distorted wave methods fro calculating collision strengths for highly charged ions, Phys. Rev. A 40 (1989) 616 – 632. `doi:10.1103/PhysRevA.40.616`.

23

[23] A. Burgess and J. A. Tully, On the analysis of collision strengths and rate coefficients, Astron. Astrophys. 254 (1992) 436 – 453.

[24] J. Oxenius, Kinetic theory of particles and photons, Springer Verlag, Berlin, 1986.

[25] I. I. Sobel'man, L. A. Vainshtein, Excitation of atoms and broadening of spectral lines, Springer, Berlin, 1998.

[26] H. Ehrhardt, K. Jung, G. Knoth and P Schlemmer, Differential cross sections of direct single elecron impact ionization, Z. Phys. D 1 (1986) 3–32.

[27] O. Zatsarinny and K. Bartschat, The B-spline R-matrix method for atomic processes: application to atomic structure, electron collisions and photoionization, J. Phys. B 46 (2013) 1 – 39. `doi:10.1088/0953-4075/46/11/112001`.

[28] M. Guerra, P. Amaro, J Machado and J. P. Santos, Single differential electron impact ionization cross sections in the binary-encounter Bethe approximation for the low binding energy regime, J. Phys. B. 48 (2015) 185202.